

## CANADIAN PARTICIPATION IN OECD/NEA-KAERI ROD BUNDLE BENCHMARK FOR CFD CODES

**J. Szymanski<sup>1</sup>, D. Chang<sup>2</sup>, D. Novog<sup>3</sup>, K. Podila<sup>4</sup>, J. Bailey<sup>4</sup>, Y. Rao<sup>4</sup>, A. Rashkovan<sup>3</sup>  
and S. Tavoularis<sup>2</sup>**

<sup>1</sup> Canadian Nuclear Safety Commission, Ottawa, Ontario, Canada

<sup>2</sup> University of Ottawa, Ontario, Canada

<sup>3</sup> McMaster University, Hamilton, Ontario, Canada

<sup>4</sup> Atomic Energy of Canada Limited, Chalk River, Ontario, Canada

### Abstract

Three submissions to the latest international benchmark exercise for computational fluid dynamics (CFD) codes used in nuclear safety applications were produced in Canada by three independently working research teams. The teams used different commercial CFD codes or code versions, different meshing tools and techniques, different turbulence modeling options and different computer resources. The paper describes the three modeling strategies and presents sample comparisons between the three solutions submitted to the blind benchmark.

### 1. Introduction

The use of CFD and its best practices in nuclear reactor safety applications is promoted internationally by the Organization for Economic Cooperation and Development (OECD) through its Nuclear Energy Agency (NEA). Among its other activities, NEA has been involved in organizing blind benchmark exercises, based on dedicated new experiments performed by recognized research organizations, producing high-quality “CFD-grade” data. The first such exercise was conducted in 2009-2010 using data from a T-junction experiment performed at the Vattenfall Research and Development laboratory at Älvkarleby, Sweden, and was deemed very successful [1]. The second exercise was launched in April 2011 and was based on new, unpublished experimental data from a rod bundle flow test, performed at the Korea Atomic Energy Research Institute (KAERI) laboratory at Daejeon, Korea.

Canada participated in the T-junction benchmark, submitting an entry produced jointly by staff of the Canadian Nuclear Safety Commission (CNSC) and nuclear safety consultants AMEC-NSS. For the purpose of participating in the KAERI rod bundle benchmark, the CNSC entered into agreements with three Canadian research organizations that expressed interest in the exercise, namely Atomic Energy of Canada Limited (AECL), McMaster University and the University of Ottawa. As a result, three different sets of CFD solutions were produced by independently working teams and submitted to the organizers by the blind benchmark deadline of May 28, 2012. This paper presents the solutions as submitted, without any insights from their comparison with the experimental data, which would be disclosed to the participants at an open benchmark meeting at a later date. Following that meeting, the participants would have a chance to work further on their solutions and perhaps improve them, but would not be able to withdraw their original submissions. Those would be processed and ranked as part of the benchmark synthesis work, with the results to be published by OECD/NEA in a report scheduled for 2013.

The organization of this paper is as follows: section 2 briefly describes the experiment, the information supplied to the participants and the benchmark submission requirements; sections 3 to 5 outline the methodologies and approaches adopted by the three research teams; section 6 presents some preliminary comparisons between the submitted solutions; and section 7 contains a conclusion.

## 2. KAERI rod bundle experiment and benchmark specifications

The subject of the benchmark exercise was a set of two dedicated tests performed at the laboratory of the Thermal-hydraulics Safety Research Division of KAERI in a facility with the acronym MATiS-H (for Measurement and Analysis of Turbulence in Subchannels – Horizontal). The description of the facility and the accompanying figures are taken from the benchmark specifications issued to the potential participants by the OECD/NEA organizers [2] and from a paper published by KAERI researchers [3].

### 2.1 MATiS-H test facility

The MATiS-H test facility is a low-temperature, low-pressure water loop with a partially transparent test section placed in a horizontal position (Figure 1). The loop is designed so as to facilitate detailed flow velocity and turbulence measurements in the subchannels of a rod bundle with a mixing-enhancing spacer grid under isothermal conditions. The test section has a square cross-section  $170 \text{ mm} \times 170 \text{ mm}$  and is nearly 5 m long. It contains a  $5 \times 5$  rod array, scaled up by a factor of 2.67 from a prototypic Pressurized Water Reactor (PWR) fuel bundle. The ratio of rod pitch ( $P=33.12 \text{ mm}$ ) to rod diameter ( $d=25.4 \text{ mm}$ ) is 1.30, which means that the spacing is not very tight. The test section hydraulic diameter ( $D_h$ ) is  $24.27 \text{ mm}$ . The loop can operate at flow rates up to about  $30 \text{ kg/s}$  and temperatures around  $35^\circ\text{C}$ , which corresponds to bulk flow velocities of less than  $2 \text{ m/s}$  and Reynolds numbers of typically about 50,000.

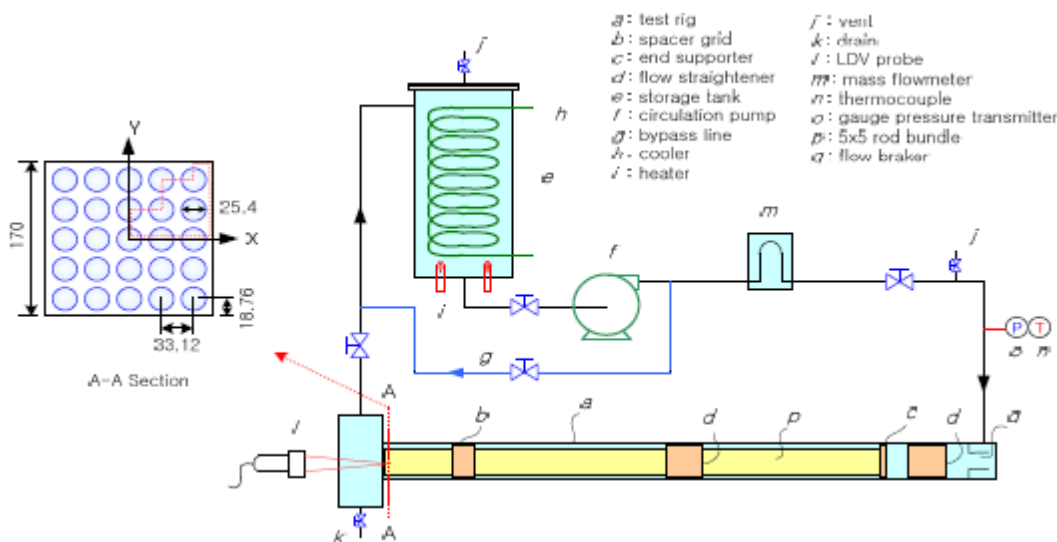


Figure 1 Schematic of MATiS-H test facility (from [2])

The outer walls of the test sections are made partly of stainless steel and partly of acrylic, to enable optical access for velocity measurements. All the internal elements, i.e., the rod bundle, the flow

straighteners and the spacer grid, are made of stainless steel. The spacer grid can be moved along the rod bundle, thus changing its distance from the fixed measurement plane downstream (A-A in Figure 1). In this way, the measurements can be performed for different locations downstream of the spacer grid (e.g.,  $1D_h$  or  $10D_h$ ). The length of the test section is sufficient to allow a distance of about  $100D_h$  between the downstream flow straightener and the spacer grid.

Detailed local velocity measurements in that plane can be performed using a variety of techniques, the principal one being two-dimensional laser Doppler anemometry (2-D LDA). The LDA probe position shown in Figure 1 is for measurements of the cross-flow velocity components  $V_x$  and  $V_y$ ; for measuring the axial component  $V_z$  the probe is placed at the side wall in plane A-A. In the latter case, the limitations of optical access due to obstruction by the steel rods cause the measurements to be restricted to the narrow gap bands between the rods (see section 2.4).

## 2.2 Spacer grid geometries for benchmark tests

The two tests performed for the benchmark exercise used two different simplified, non-proprietary spacer grids, one with so-called split-type vanes and the other with swirl-type vanes (Figure 2).

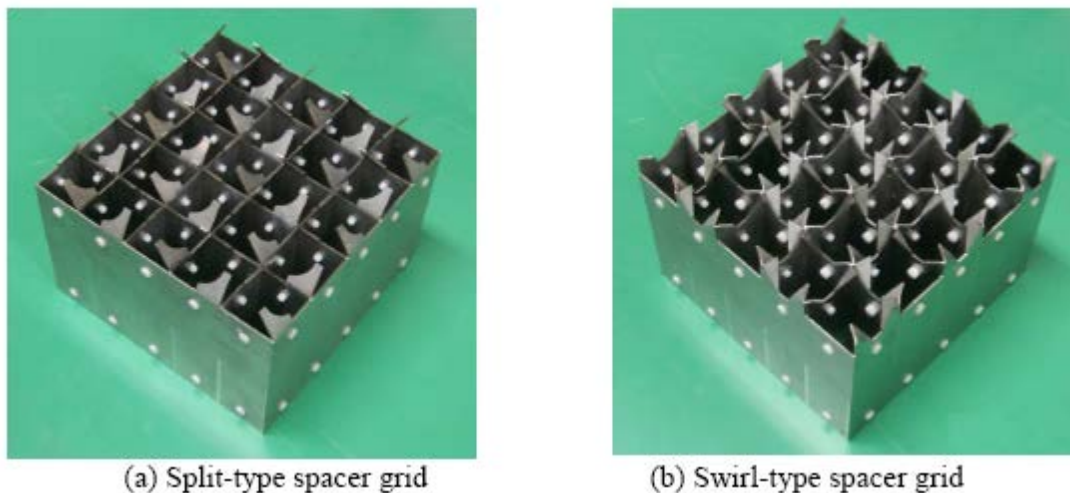


Figure 2 Test spacer grids used in the experiment (from [2])

The geometry data for the spacer grids were made available to the exercise participants in the form of detailed design drawings included in the benchmark specifications [2], and also in the form of computer-aided design (CAD) data files produced using CATIA 5 software.

## 2.3 Benchmark test conditions

The target loop parameter values are identical for both benchmark tests, matching the conditions during an earlier test with a bare bundle (with no spacer grid), performed specifically for the purpose of providing inlet boundary conditions for the benchmark predictions (see next section). The mass flow rate is 24.2 kg/s, the temperature is 35°C, and the pressure is 156.9 kPa(a). This results in a bulk flow velocity of 1.50 m/s and a Reynolds number of 50,250 [2].

## **2.4 Inlet boundary conditions**

The test section was designed so as ensure fully developed bare bundle flow conditions just upstream of the spacer grid, i.e., about  $100D_h$  downstream of the second flow straightener. To confirm this, a test with no spacer grid was performed before the benchmark and its results were provided to the participants for possible use as inlet boundary conditions. The benchmark organizers suggested that this data be used to specify inlet boundary conditions at about  $10D_h$  upstream of the spacer grid; however, the data proved to be of limited use for that purpose because of the incomplete flow field coverage, and other means of formulating inlet boundary conditions had to be devised (see sections 3, 4 and 5).

## **2.5 Data requested for benchmark submission**

The organizers requested that the participants submit their calculated results for at least one type of spacer grid (split-type recommended), but preferably for both. The data had to be submitted as a precisely defined set of files with prescribed names and formats to facilitate uniform and at least partly automated processing of the submissions.

The main body of requested data included time-averaged values of three velocity components and their root-mean-square fluctuations at four cross-planes, located  $0.5D_h$ ,  $1.0D_h$ ,  $4.0D_h$  and  $10.0D_h$  downstream of the spacer grid exit plane. It also included the values of mean velocity circulation in one specified subchannel of the bundle, calculated by integrating the axial component of rotation over the entire subchannel area, at the same four planes.

In addition to the basic data, the organizers requested a characterization of the CFD methodology and meshing in an accompanying document. The information requested included the order(s) of the numerical scheme(s), the total number(s) of volumes used in the calculations, the range(s) of wall-normal coordinate  $y^+$ , the minimum and maximum cell edge length(s), details of the turbulence model used, computer resources and calculation time(s).

## **3. Benchmark submission produced by AECL**

The submission from AECL included only one solution, for the split-type spacers. The continuity and Navier-Stokes equations for isothermal, incompressible and constant density flow problem were solved using a general purpose commercial CFD code, ANSYS Fluent 6.3.26. ANSYS meshing software was utilized for meshing the  $5 \times 5$  rod bundle.

The fluid domain was divided into three main zones: the upstream zone, the spacer zone and the downstream zone. No symmetry or periodic boundary conditions were employed to preserve the ability to resolve all possible vortex structures downstream of the vanes. For the initial base-case computations, a paved, primarily quadrilateral mesh (some triangular cells were generated to improve quality) was placed on each of the faces between the spacer and upstream and downstream zones. These surface meshes were then extruded as hexahedral elements (or triangular prismatic elements in the case of the triangular surface cells) to the extent of the upstream and downstream zones. The spacing for the upstream extrusion was set at 5 mm, while the spacing for the downstream extrusion, where the data was to be taken, was set at 3 mm. The spacer zone was meshed with patch conforming tetrahedrons with a minimum allowable cell edge size of 0.1 mm and

a maximum allowable cell edge size of 4 mm. In addition to the tetrahedral cells, this produced some pyramidal and wedge cells at the interface with the quadrilateral surface mesh adjoining the other zones. The computational base-case mesh was refined by adapting to the velocity gradients in the downstream section, resulting in a final mesh count of 15.3 million cells, ( $y^+ = 30$ , almost everywhere), which was close to the available hardware capacity limit. Solution was obtained using the unsteady Reynolds-averaged Navier-Stokes (URANS) approach in conjunction with the Reynolds stress turbulence model (RSM). RSM solves differential transport equation for each Reynolds stress component, and is capable of resolving anisotropic behaviour better than two-equation models based on the Boussinesq eddy-viscosity approximation. The model constants present in the RSM were not modified, and standard wall functions were used to resolve the fluid flow in the near wall region.

The solver selected for this study was a segregated solver based on the point Gauss-Seidel technique with multigrid V-cycle acceleration. The under-relaxation factors were reduced for momentum and Reynolds stresses (0.5 and 0.25 respectively) to improve the solution convergence. To ensure full convergence, residuals for continuity, momentum and stress components were converged below a value of  $10^{-5}$ . In order to reduce run time, the current investigation used first-order upwind schemes for the convective terms. The temporal discretization was achieved using first-order implicit time differencing scheme built-in in ANSYS Fluent. The semi-implicit pressure-linked equations (SIMPLE) algorithm was employed for pressure-velocity coupling. The simulations performed at AECL used uniform inlet boundary condition at the MATiS-H's entrance region with the axial velocity of 1.5 m/s based on the benchmark specifications [2]. A turbulence intensity of 5% was used at the inlet. The simulations were performed using 3D double-precision parallel solver running on a Hex core HP Z800 workstation with 64 GB of RAM and 1 TB hard drive, operating under Red Hat Linux. The running time for the final run was about 14 days (336 hours).

#### **4. Benchmark submission produced by McMaster University**

The procedure for producing the final submission from McMaster University comprised two stages. First, turbulence model and mesh sensitivity studies on various partial geometries were carried out. This stage was concluded by performing a series of comparisons with previously published experimental results on a similar setup [5, 6]. Based on the comparisons, the final simulation scheme was chosen for the benchmark submission.

Early on in the sensitivity study stage, attempts were made to run steady calculations with three Reynolds-averaged Navier-Stokes (RANS) turbulence models incorporated in the commercial CFD code STAR-CCM+, namely realizable  $k-\epsilon$  (RKE), shear stress transport (SST)  $k-\omega$ , and Reynolds stress model (RSM). The geometry chosen was that of the infinite bundle (infinitely periodic in the cross-sectional plane). Hence, no effects of the test section walls were taken into account.

The “all  $y^+$ ” wall treatment was employed throughout the computation domain with uniformly built boundary layers. The boundary layer was built in such a way as to assure  $y^+$  of the order of unity on the walls. In these runs, the RKE model converged to a steady solution, while RSM diverged in a non-fluctuating manner. The SST  $k-\omega$  model did not lead to a converged solution, but rather the residuals and some local velocity monitors were fluctuating in a regular way. The SST  $k-\omega$  model solution suggested that transient behaviour and vortex shedding from the centralizing buttons should be anticipated. In view of this, a transient procedure was employed for the geometry containing only one centralizing button, without vanes on top of the grid (Figure 3).

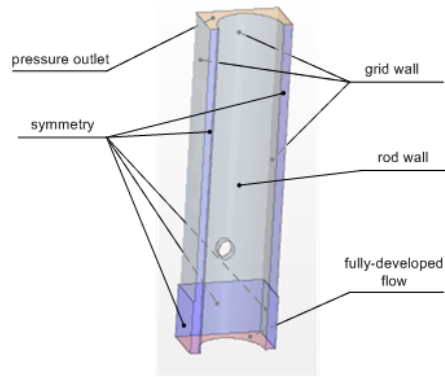


Figure 3 Computational domain for studying flow past centralizing buttons

Only the SST  $k-\omega$  model led to a converged periodic solution that showed vortex shedding. The results were verified with two different meshes and two time steps. The shedding frequency appeared to be about 30% higher than in the case of an equal diameter cylinder in the free stream for the equivalent average velocity. No converged transient solution was achieved with the RSM model. The RKE model did show some non-periodic transient structures with very low amplitude, and thus was not considered as converged. Additional runs using infinite bundle with mixing vanes but without buttons showed no transient behaviour in the entire flow domain. Thus it was concluded that the centralizing buttons are responsible for the majority of the transient flow behaviour in the limit of the models tested. Further infinite bundle tests revealed that using a coarse mesh in the buttons region and a fine mesh downstream led to a converged steady solution. Given that real bundle analyses may involve heat transfer and non-constant fluid properties, the computational advantages of RANS, relative to unsteady simulations, become significant. Hence the McMaster team decided to go forward with RANS modeling for the remainder of the benchmark, and to deploy mesh-based filtering in the regions of highly unsteady behaviour.

An infinite bundle model was also used for mesh sensitivity studies. Three different core meshes were used for the infinite bundle with the split-vane grid. Boundary layers were the same for the three core meshes studied in order to limit the effect of the chosen wall treatment on the final solution. As a result of this approach, the appropriate core mesh was selected. No attempts were made to further optimize the meshing, e.g. by using gradient-adaptive procedures.

A further sensitivity study was performed to examine the effects of the complicated outlet geometry on the flow near the grid plates. The outlet plenum, where the flow from the rectangular 170x170 mm bundle was divided into three 120° separated outlet pipes, was modelled downstream of the test section. This model was intended to mimic the exact test geometry. It was found that no appreciable effect of the outlet on the flow field in the measuring plane was to be expected. At this stage the computational scheme was frozen.

The final tests of the turbulence model and the grid quality were done by simulating the reported 2008 tests by KAERI [5, 6] and comparing the predictions with the published experimental results. The geometry of the rod bundle with a split-vane grid and experimental conditions of the tests reported in 2008 were very similar to the ones to be submitted for the present benchmark. It was found that realizable  $k-\epsilon$  model resulted in the best comparisons with the published data. Core mesh size chosen after the infinite bundle tests was found to be appropriate also for the finite bundle, where the 170x170 mm channel wall effects are inherently present.

Both flows in the actual 5×5 rod bundle benchmark geometries with the split and the swirl vane grids were simulated using the RKE model incorporated in STAR-CCM+ with default values of all parameters. The individual Reynolds stresses were calculated from the turbulent kinetic energy with the use of the Boussinesq isotropic eddy viscosity hypothesis. The simulated geometries included a 2 m long ( $\sim 82D_h$ ) bare-bundle upstream flow development region. The inlet velocity was specified as uniform and the inlet turbulence intensity as 5%; the pressure boundary condition was specified at the outlet. A trimmer mesh with prism layers for the wall layer, with about 63 million cells and  $y^+$  ranging from 0.04 (at the tips of the spacer vanes) to 1.8 was used. A 2nd-order upwind numerical scheme was used for the convective term. The SIMPLE algorithm was used for the treatment of pressure-velocity coupling. The simulations took about 30 hours clock time per case on a computer system containing 32 processors (2GHz x86-64 CPU) with 64 GB of memory, running under Linux (Centos 5.5, kernel version 2.6.18).

## 5. Benchmark submission produced by the University of Ottawa

The University of Ottawa team completed unsteady simulations for both the split-type and the swirl-type spacer grids. The computational domain was divided into four sub-domains as shown in Figure 4: an upstream rod-bundle zone with a length of  $10.0D_h$ ; a grid zone with a length of  $4.3D_h$ ; a spacer zone with a length of  $0.8D_h$ ; and a downstream rod-bundle zone with a length of  $12.0D_h$ . The entire cross-section of the rod bundle was modelled, and no assumption of flow symmetry was employed.

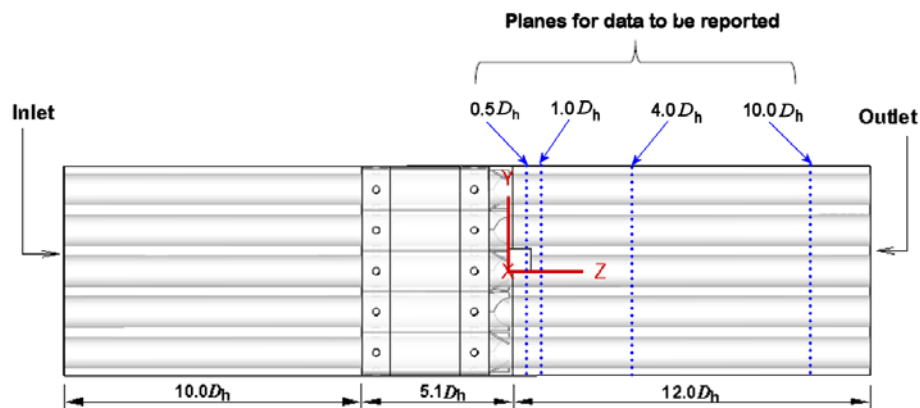


Figure 4 CFD model for the rod bundle array with spacer grids

Tetrahedral meshes were used in the two grid button sub-domains and the spacer grid sub-domain, while hexahedral meshes were used in the upstream and downstream rod bundle domains, as well as in the middle section between the two grid button sub-domains. To account for the geometric complexity of the grid buttons and the vanes, a tetrahedral rather than hexahedral mesh was chosen, because the latter had a lower mesh quality. To resolve the steep velocity gradients near walls, prismatic elements were allocated in boundary regions, with 20 prism layers across each boundary region. To examine the effect of mesh size for numerical verification, steady RANS simulations with the re-normalization group (RNG)  $k$ - $\epsilon$  turbulence model were conducted for the split grid spacer configuration with four different meshes (7, 11, 13, and 19 million cells). The differences between axial velocity and turbulent kinetic energy profiles between the mesh with 13 million cells and the mesh with 19 million cells were less than 5%. This test indicated that an acceptable level of



mesh convergence was achieved for steady RANS simulations. Further numerical verification was conducted using unsteady hybrid simulations. Comparisons were made between results with 19 million cells and 22 million cells. The latter mesh was obtained by doubling the number of cells in the cross-section of the downstream rod-bundle zone while keeping the same mesh spacing in the streamwise direction. Noticeable differences were found in the RMS velocity fluctuations. Therefore, the mesh with 22 million cells was selected for the split-type spacer configuration. The mesh size for the swirl-type spacer had 20 million cells.

The simulations of flows in the rod bundle with spacer grids were of a segregated-hybrid type, consisting of a combination of scale-adaptive simulations (SAS) and large-eddy simulations (LES). SAS was used in the upstream rod-bundle sub-domain and the spacer grid sub-domains, whereas LES was used in the spacer vane sub-domain and the downstream rod-bundle sub-domain. In the interface between the SAS and the LES and in the inlet plane, the velocity fluctuations were modeled by using the synthetic eddy method (SEM), also called the vortex method, to specify time-varying velocity fluctuations [7]. The SAS introduces source terms in the  $\omega$  equation in terms of the von Kármán length scale, which is the ratio of the first and the second velocity gradients. The SAS acts like LES in unsteady regions where the von Kármán length scale is relatively small, while it works as URANS with the SST model in the steady regions where the von Kármán length scale is increased [8]. The wall-adapting local eddy-viscosity (WALE) model [9] was chosen as a subgrid model for the LES because this subgrid model is capable of predicting correctly the asymptotic flow behaviour near the wall in wall-bounded turbulent flows.

The simulations employed the second-order central difference scheme for the convection terms of the transport equations. The second-order implicit Euler scheme was employed for temporal discretization. To avoid numerical instability caused by the combination of high-aspect ratio grid cells and highly-clustered near-wall spacing, the SIMPLEC (semi-implicit pressure-linked equations – consistent) algorithm was used for the treatment of pressure-velocity coupling.

Because measurements in the bare rod bundle that were meant to serve as inlet conditions were provided only for parts of the cross-section and did not cover the entire inlet plane, these data could not be used. Instead, steady RANS simulations with the RSM model were conducted for a bare rod bundle array with a length of  $95D_h$  to obtain the velocity and the Reynolds stress distributions in the entire inlet plane for the spacer grid simulations. In the bare-bundle simulation, the outflow boundary condition with zero diffusion flux was imposed at the outlet. All simulations were conducted using the commercial CFD package ANSYS FLUENT 13 on 64-bit Linux servers with 6 Quad core 6234 processors operating at 2.4 GHz and with 64 GB RAM. 47 threads of CPU processors were used for the computations. The total computational times were 2,463 hrs for the split-type spacer simulations and 1,638 hrs for the swirl-type spacer simulations.

## 6. Comparison of submitted predictions

Before discussing the results of the present analyses, it seems worthwhile to view the adopted computational procedures within the context of general CFD methodologies for industrial flows. As far as solution accuracy is concerned, Direct Numerical Simulation (DNS), an approach that solves numerically the equations of motion without modelling, would have been the method of choice, but it has long been realized that DNS is not feasible for high Reynolds number turbulent flows because of the extremely large computational resources (fine mesh, small time step and high-order discretization scheme) required to capture turbulent motions to the smallest dynamically important



scale (Kolmogorov microscale). All other methods are based on the modelling of some or all turbulent motions. A widely used CFD method for industrial flows is the solution of the Reynolds-Averaged Navier Stokes (RANS) equations, coupled with modelled equations for the turbulence. This method has the lowest requirements in terms of computational time and computer size, but its accuracy depends on the geometry and flow conditions, as well as the turbulence model capabilities. Moreover, RANS methods cannot resolve time-dependent motions. Unsteady RANS (URANS) methods maintain the turbulence modelling used in RANS, but can also resolve time-dependent large-scale motions, if such are present in the flow. URANS require significantly larger computational time than RANS and would produce the same solutions as RANS in flows in which unsteady effects are not significant. Large Eddy Simulations (LES) solve low-pass filtered dynamic equations, so that motions with a scale smaller than a specified value (sub-grid-scale motions - SGS) are not resolved but taken into consideration in the solution with the use of an SGS model. The filter cut-off scale must be within the inertial spectral subrange, which can be quite small in high Reynolds number turbulent flows, especially near walls. Thus, mesh size and time step must be sufficiently small for LES to work. Coarse LES would miss a significant part of the turbulence activity and could also suffer from other unpredictable inaccuracies due to the inapplicability of the SGS model. A host of hybrid methods, combining LES and URANS or otherwise simplifying LES solutions in at least some parts of the computational domain, have been introduced in an effort to maintain the accuracy of LES at a lower computational cost.

As mentioned in section 1, the Canadian MATiS-H benchmark participation project was not aimed at combining efforts of its individual participants to produce a single submission, but instead allowed each of the teams to select their own modeling approach, based on their expertise, technical judgment and available resources. As a result, the three submissions have a few commonalities, such as the use of currently available commercial CFD codes run on Linux workstations, but differ significantly in a number of modeling essentials, representing the range of CFD techniques currently used for simulating turbulent flows in practical industrial applications. The most important characteristics of the submissions for the split-vane spacer geometry are compared in Table 1.

Organi- zation	Code	Turbu- lence model	Mesh size (million)	Convective term scheme	Time- marching scheme	Computer resources	CPU time (hrs)
McMaster University	STAR- CCM+	RANS – RKE	63	2 <sup>nd</sup> order upwind	Steady-state solution	32 CPU cluster	32
AECL	ANSYS Fluent 6.3.26	URANS – RSM	15	1 <sup>st</sup> order upwind	1 <sup>st</sup> order implicit	HP Z800 workstation (6 cores)	336
University of Ottawa	ANSYS Fluent 13	Hybrid SAS/ LES	22	2 <sup>nd</sup> order central	2 <sup>nd</sup> order implicit	6 CPU server (48 threads)	2463

Table 1 Specifications of the three Canadian submissions for the split-vane case

The order-of-magnitude differences in the computing times are attributable mainly to the use of different turbulence models and the related choice of steady or unsteady simulation. A steady RANS simulation with the relatively simple and robust realizable  $k-\epsilon$  model is clearly the least computationally demanding. Run on a cluster of 32 CPU workstations, it produced a solution on a

large mesh within a day or so. In contrast, the transient models required running times of weeks or months, partly because the transients needed to be run for long enough simulation times so that time-averaged quantities achieved statistical independence of the averaging time. The URANS approach using RSM, with a relatively small mesh size, required a run time of about two weeks on a relatively modest 6-core workstation. The hybrid SAS/LES approach was, as expected, the most computationally intensive, requiring a run time in excess of three months on a 24-core workstation cluster.

Selected samples of the results submitted by the three benchmark teams for the split-type spacer grid geometry are presented in Figures 5 to 7. It can clearly be seen that the three predictions show significant differences. The axial velocity predictions (Figure 5) display similarities in terms of general trends and character of variability, but the maxima and minima do not always coincide and their values differ significantly. The RANS show the highest variability and the URANS the lowest one. Differences in the predictions of the RMS velocity fluctuations are even more pronounced, both in terms of extreme values and the overall turbulence levels (Figures 6 and 7). The reported LES simulations employed the finest mesh permitted by the computer used at that time for mesh generation and it turned out that the spanwise and streamwise grid spacing did not entirely satisfy the LES meshing criterion. As a result, the reported turbulence values are likely to be underestimates, as a non-negligible part of turbulent motions would be spatially filtered out. Preliminary results of further refined LES simulations (40 million mesh elements) indicate significantly higher turbulence stresses in the subchannel gap regions than those reported here. Figures 6 and 7 also show that URANS turbulence predictions are much lower in level than the other two. This discrepancy is attributed to a combination of effects, the most significant of which seems to be the usage of insufficient mesh count.

The differences in the predictions are being analyzed and explanations for them are being sought in the open phase of the exercise, which is currently underway, and in a broader context of all blind benchmark submissions in the exercise synthesis performed by KAERI.

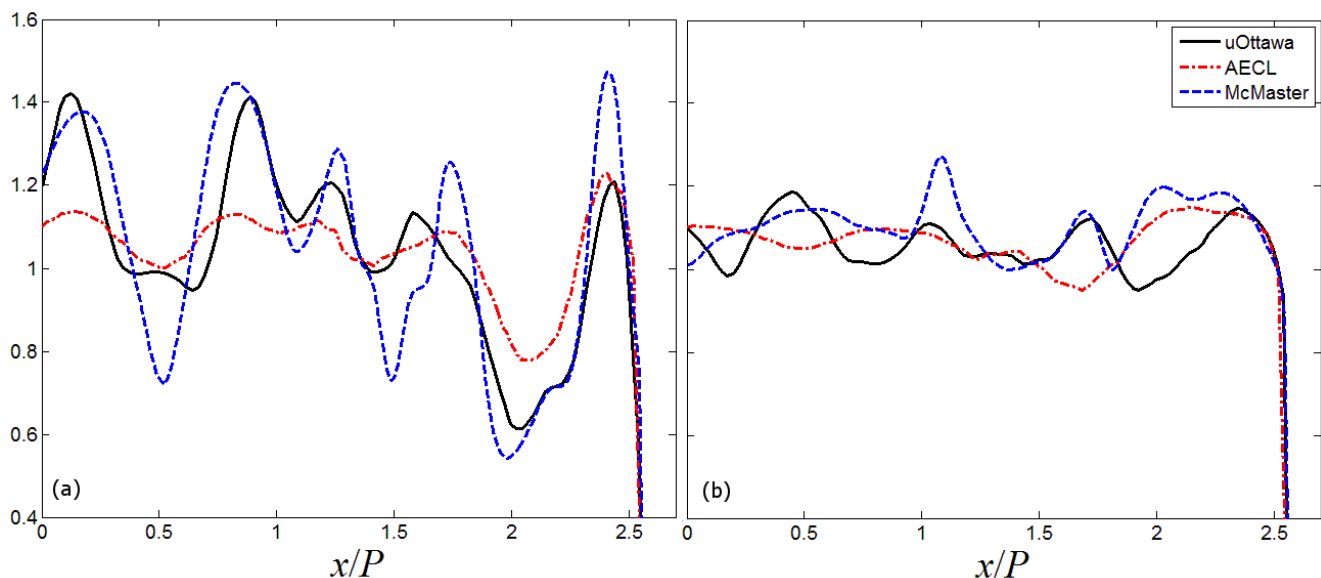


Figure 5 Axial velocity ( $W$ ), normalized by bulk velocity, at  $y/P = 0.5$ : (a)  $z/D_h = 1.0$  and (b)  $z/D_h = 4.0$  ( $P$  – tube pitch; see Figure 1 for the coordinate system)

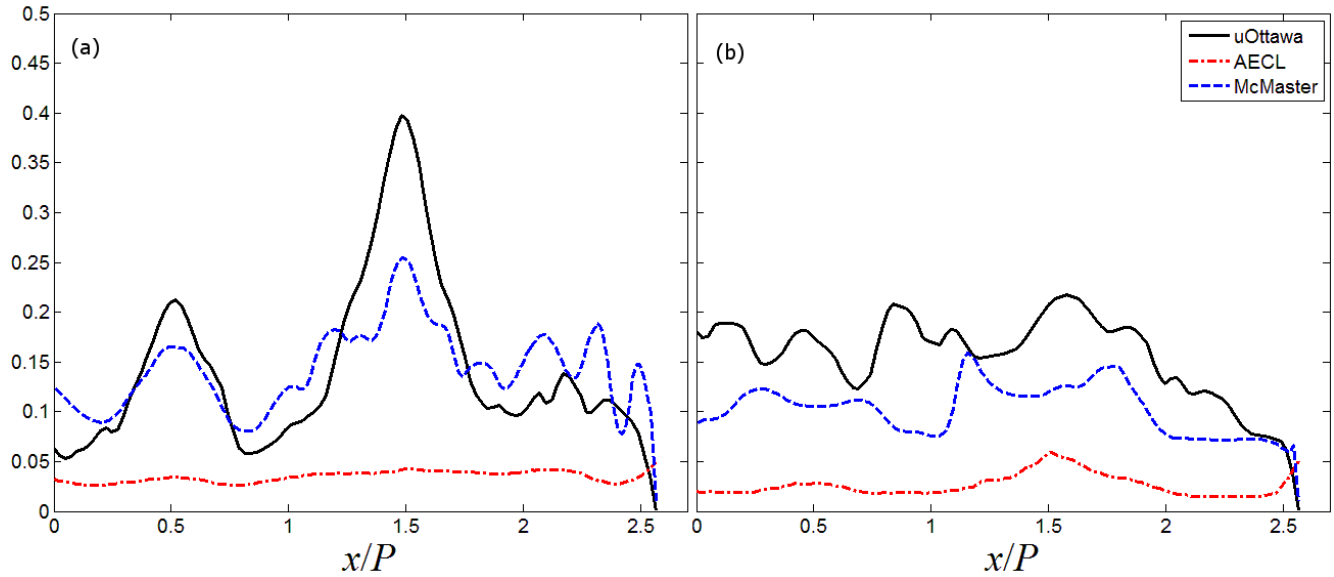


Figure 6 Spanwise RMS velocity fluctuations ( $u$ ), normalized by bulk velocity, at  $y/P = 0.5$ :  
(a)  $z/D_h = 1.0$  and (b)  $z/D_h = 4.0$

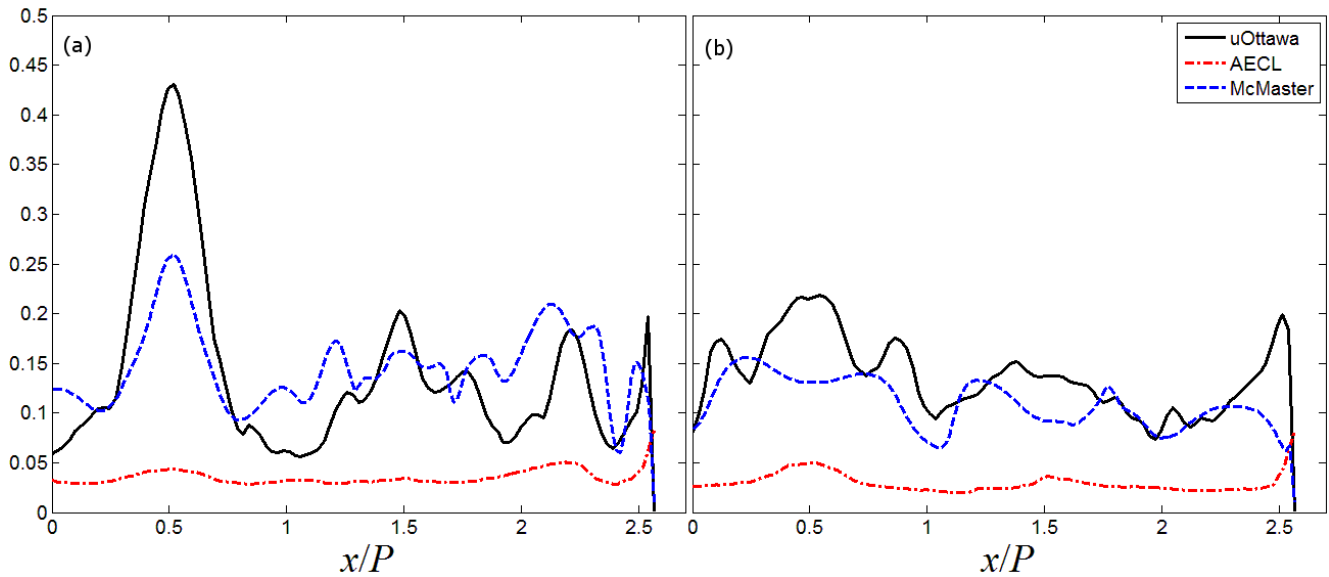


Figure 7 Transverse RMS velocity fluctuations ( $v$ ), normalized by bulk velocity, at  $y/P = 0.5$ :  
(a)  $z/D_h = 1.0$  and (b)  $z/D_h = 4.0$

## 7. Conclusion

The first, blind phase of the international CFD benchmark based on the MATiS-H rod bundle experiments has been successfully completed. Three Canadian teams submitted their predictions after performing independent simulations using two different commercial CFD codes and three different modelling approaches to predict time-averaged fluid flow and turbulence characteristics. The three submissions show significant differences in predictions for the same flow conditions.

These differences are being investigated in the second, open phase of the exercise through comparisons with experimental data released by KAERI.

## 8. References

- [1] B. L. Smith, J. H. Mahaffy and K. Angele, “A CFD benchmarking exercise based on flow mixing in a T-junction”, Proceedings of the 14th International Topical Meeting on Nuclear Reactor Thermalhydraulics, NURETH-14, Toronto, Ontario, Canada, September 25-30, 2011.
- [2] “OECD/NEA—MATiS-H Benchmark Final Benchmark Specifications”, attachment to e-mail from [Abdallah.AMRI@oecd.org](mailto:Abdallah.AMRI@oecd.org), February 28, 2012.
- [3] Kang, H. S., Chang, S. K. and Song, C.-H., “CFD analysis of the MATIS-H experiments on the turbulent flow structures in a rod bundle with mixing vanes”, Proc. CFD4NRS-3, Washington, D.C., USA, Sept. 14-16, 2010.
- [4] McClusky, H. L., Holloway, M. V., Beasely, D. E., Conner, M. E., “Development of Swirling Flow in a Rod Bundle Subchannel”, *Journal of Fluids Engineering*, Vol. 124, 2002, pp 747-755.
- [5] Chang S.K., Moon S.K., Baek W.P. and Choi Y.D., Phenomenological investigation on the turbulent flow structures in a rod bundle array with mixing vanes, *Nuclear Engineering and Design*, 238(2008), 600-609.
- [6] Chang S.K., Moon S.K., Baek W.P. and Chun T.H., The experimental study on mixing characteristics in a square subchannel geometry with typical flow deflectors, *Heat Transfer Engineering*, 29(2008), 695-703.
- [7] M.E. Sergent, “Vers une Méthodologie de Couplage Entre la Simulation des Grandes Echelles et les Modèles Statistiques”, Phd Thesis, Ecole Central de Lyon, 2002.
- [8] F.R. Menter and Y. Egorov, “A scale-adaptive simulation model using two-equation models”, 43th Aerospace Science Meeting and Exhibit, AIAA paper 2005-1095, Reno, NV, USA, 2005.
- [9] F. Nicoud and F. Ducros, “Subgrid-scale stress modelling based on the square of the velocity gradient tensor flow”, *Turbulence and Combustion*, Vol. 62, 1999, pp. 183–200.